Biomimetic sensor based on Mn(III) *meso*-tetra(N-methyl-4-pyridyl) porphyrin for non-enzymatic electrocatalytic determination of hydrogen peroxide and as an electrochemical transducer in oxidase biosensor for analysis of biological media.

Ruiqin Peng[1], Andreas Offenhäusser[1], Yuri Ermolenko[2], Yulia Mourzina[1]*

[1] Institute of Biological Information Processing (IBI-3, Bioelectronics), Forschungszentrum Jülich, 52425, Jülich, Germany

[2] Institute of Chemistry, Saint Petersburg State University, Universitetskaya nab. 7/9, 199034 Saint Petersburg, Russia

*Corresponding author: y.mourzina@fz-juelich.de (Dr. Yulia Mourzina)

Abstract: Bioinspired molecular complexes that mimic the enzymatic catalysis of redox transformations offer a versatile platform for the development of non-enzymatic mediatorless sensors with high sensitivity, selectivity, and robustness without the use of precious metals. The aim of this study was to prepare and investigate biomimetic sensors based on the electrocatalytic reduction of hydrogen peroxide and oxygen by a series of immobilized complexes of iron and manganese with porphyrin macrocycles for the detection of hydrogen peroxide and glucose. The influence of substitution of the macroheterocyclic ligand, composition of the adsorption solution, Nafion membrane, and amino acids on the properties of the sensors was studied. Optimized sensor function is based on the electrogenerated reduced form of Mn(II) *meso*-tetra(N-methyl-4-pyridyl) porphyrin as a catalyst and allows high sensitivity of the hydrogen peroxide detection of 1.8 A M^{-1} cm^{-2} and 0.071 A M^{-1} cm^{-2} to be achieved in the lower and higher concentration ranges, respectively, with a low detection limit of $5 \cdot 10^{-7}$ M at physiological pH 7.4 and in the presence of oxygen. The MnTMPyP electrode was investigated as an electrochemical transducer in the glucose-oxidase-based biosensor. The sensors were successfully applied for the detection of hydrogen peroxide and glucose in human serum samples. Along with a simple fabrication procedure and robustness of the sensor, the biomimetic electrocatalytic properties of the MnTMPyP complex facilitate excellent performance of the proposed sensors for hydrogen peroxide and glucose determination in biological media, emphasizing the importance of bioinspired electrocatalytic metalloporphyrin complexes for the development of sensors and point-of-care devices.

Keywords: manganese porphyrin, biomimetic sensor, electrocatalysis, hydrogen peroxide, glucose oxidase, iron porphyrin

1. Introduction.

Electrochemical sensors and systems with hydrogen peroxide are an important topic in current scientific investigations because of the established role of hydrogen peroxide in diverse fields. In biological systems, it is involved in redox signaling [1-3] and ROS-based medicine [4]. In cells, where most hydrogen peroxide is generated through the dismutation of the superoxide radical anion originating mainly from the electron transport chain of aerobic respiration, it also contributes to oxidative stress conditions responsible for toxic effects, which damage cell components, and is also involved in a number of diseases and pathologies [1]. Furthermore, hydrogen peroxide is a redox-active product of the metabolic redox reactions catalyzed by oxidase enzymes (e.g., glucose oxidase, monoamine oxidase, glutamate oxidase). Consequently, determination of hydrogen peroxide is a strategy for the determination of glucose, monoamines, glutamate, lactate, and cholesterol. Along with its role in biological processes, hydrogen peroxide is of great interest for industrial, ecological, and analytical applications [5-8].

These topics have motivated significant research activity in the development of sensors for hydrogen peroxide determination in various media [3, 9-18]. Electrochemical sensors based on modified electrodes are often the method of choice due to their widely recognized advantages such as accuracy, miniaturization potential, low costs, simple instrumentation and utilization, portability, temporal resolution, and applicability for real-time measurements and implantation. Modern electrochemical sensors for hydrogen peroxide rely on bio- and electrocatalytic reactions on the electrode surfaces modified with peroxidase enzyme, smaller biomolecular catalysts (e.g., cytochrome *c*, myoglobin) [10, 12, 19], noble metals, oxides, metal and carbonaceous electrode nanomaterials [11, 13-15, 20-22], as well as their synergy [12, 23-25]. Modifying the electrodes makes it possible to decrease the overpotential of the hydrogen peroxide reduction or oxidation, increase currents, and improve the selectivity of the determinations.

The development of non-enzymatic sensors based on biomimetic molecular complexes is expected to make use of the synergic effect of the above-mentioned materials and combine their advantages, while being at the same time more robust, flexible, easy-to-use, and not consuming noble metals [9, 26-30]. In natural redox biological transformations, metalloproteins with iron, copper, and Fe/Cu active site tetrapyrrolic complexes mediate oxygenation reactions

with oxygen and hydrogen peroxide terminal oxidants [31]. By analogy with natural systems, a biomimetic electrocatalytic reduction of hydrogen peroxide using metal complexes with N_4-macoheterocycles as electrocatalysts is a candidate for the development of electrochemical sensors for hydrogen peroxide [9]. Along with the central metal of the complex, substituents of the tetrapyrrolic macroheterocycle may contribute to the redox properties of the complex as well as steric interactions and arrangements, which makes it possible to modify the sensor properties with respect to detection limit, sensitivity, and selectivity [32]. As far as hydrogen peroxide sensing is concerned, most work has been performed with iron porphyrin complexes, since these macroheterocycles are direct analogues of the hemes in HRP, cyt *c*, and other redox hemoproteins. There is also growing interest in manganese porphyrins as biomimetic components and sensor materials in electrochemical and electrocatalytic systems because of the essential role of manganese in redox biological processes in photosystem II and non-heme manganese catalase enzymes, the possibility of tuning the environment of the central metal ion, the ability of the manganese ion to change oxidation states, and its interactions with various oxygen-containing species such as oxygen, superoxide, and hydrogen peroxide [33, 34]. Moreover, manganese porphyrins may be advantageous in comparison with Fe and Cu porphyrin complexes for the construction of *in vivo* sensors and with respect to applications in biological systems, since Fe and Cu porphyrin complexes have been shown to participate in the Fenton reaction, react with H_2O_2 to form $HO^{\bullet}$, inducing cell death, being cytotoxic [35]. Unlike Fe and Cu porphyrins, MnTMPyP does not participate in the Fenton reaction and does not exhibit cytotoxicity. However, unlike the iron and cobalt complexes, only a few examples of manganese macrocycles have been reported as catalysts of the molecular oxygen reduction reaction, the epoxidation reaction, as well as the superoxide dismutase mimic, and as scavengers of the reactive oxygen species [8, 35-39]. However, it has been assumed that biomimetic iron and manganese complexes have similar intermediates in the reaction with oxygen and incompletely reduced oxygen species [39]. It has been shown that manganese tetrakis(sulphonatophenyl)porphyrin complex has a higher peroxidase-like activity in the spectrophotometric determination of hydrogen peroxide than a number of Fe-, Co-, Cu- Zn- and metal-free porphyrins [40].

Recently we performed an investigation on a series of water-soluble manganese porphyrins in the electrocatalytic reduction of oxygen and hydrogen peroxide in aqueous solutions, where the electrode support did not essentially influence the redox properties of the complexes, and where we discussed possible intermediates and mechanisms of the reactions [41]. This study revealed prospects of the Mn(III) *meso*-tetra(N-methyl-4-pyridyl) porphyrin

complex for the biomimetic electrochemical sensing of hydrogen peroxide based on the electrocatalytic reduction reaction. However, the distinction in the properties of metal complexes with tetrapyrrolic ligands in the bulk dissolved and adsorbed states suggest a difference in their electrocatalytic properties and is worth investigating [42-45]. To the best of our knowledge, this is the first detailed study of the sensor based on the electrocatalytic properties of the Mn porphyrin in reduction of hydrogen peroxide as applied for the analysis of biological media. In this investigation, we study and compare the immobilization and biomimetic sensor properties of complexes of Mn and Fe with porphyrin macrocycles for a non-enzymatic selective electrocatalytic determination of hydrogen peroxide. Properties of the modified electrode as an electrochemical transducer for the oxidase biosensor and an analysis of biological media are also shown and discussed.

2. Experimental

2.1. Materials and solutions.

Mn(III) *meso*-tetraphenylporphine chloride, MnTPP, Mn(III) *meso*-tetra(N-methyl-4-pyridyl) porphine pentachloride, MnTMPyP, Fe(III) *meso*-tetra(N-methyl-4-pyridyl) porphine pentachloride, Fe(III)TMPyP, and Fe(III) *meso*-tetraphenylporphine chloride, Fe (III)TPP with a purity of >95 % were purchased from Frontiers Scientific Inc., Figure 1. All other chemicals of analytical reagent grade, Nafion solution (5 wt. % in mixture of lower aliphatic alcohols and water), glucose oxidase from *Aspergillus niger* (145200 U/g), and human serum were supplied by SigmaAldrich. Solutions of the interfering species including ascorbic acid, uric acid, glutamic acid, aminobutyric acid, glucose, and dopamine in phosphate buffer (pH 7.4, 0.1 M) were prepared before use. Glucose solution was allowed to mutarotate overnight at room temperature before use. Glucose solutions were then stored at 4 C°. The 0.1 M phosphate buffer solutions, PBS, were prepared from NaH_2PO_4 and Na_2HPO_4. The pH was controlled by the laboratory pH meter 765 (Knick GmbH). All aqueous solutions were prepared using deionized water.

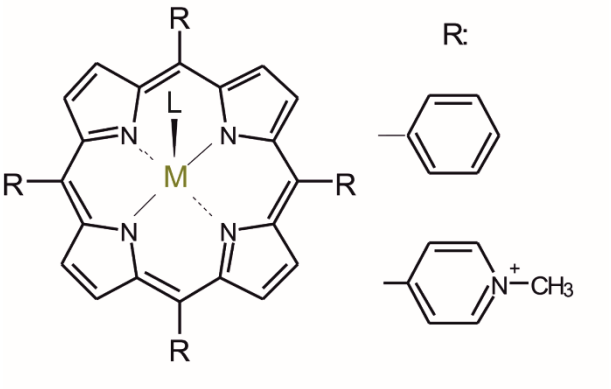

Fig. 1. Metalloporphyrin complexes, M: Fe(III) and Mn(III). L may denote the aqua and hydroxo-ligand as well as the GCE surface.

2.2. Electrode cleaning and functionalization.

The glassy carbon electrodes were polished by diamond (1 μm particle size) and alumina (0.05 μm particle size) polishing suspensions. The polished electrodes were washed in ethanol for 10 min and in pure water for 30 min. Then, the electrodes were treated by ultrasound for 10 seconds in water, washed and dried by a stream of air. After the cleaning procedure, the electrodes were immersed into solutions of the metalloporphyrin complexes for 24 h and then dried at room temperature. Subsequently, 10 μL of different concentrations of the Nafion solution in DMF was dropped onto the surface of the electrodes and the electrodes were left to dry at room temperature. The electrodes were stored at room temperature in dry conditions and soaked in the PBS for 10 min before use.

Electrode functionalization with metalloporphyrin and glucose oxidase was performed based on previous studies [24, 46] using two different procedures, which are described in the supporting information, Section S2.

2.3. Electrode cleaning after immobilization.

A number of cleaning procedures were tested for the GCEs after immobilization of the porphyrins, including various solvents such as DMF, chloroform, and 2 % Helmanex III. The procedure finally established was as follows. First, the membrane was removed by washing with ethanol and water, and using the filter paper. Then, the electrodes were washed in ethanol for 15-20 min while the solvent was stirred followed by ultrasonication in ethanol for 8-10 s. After that the electrodes were washed with ethanol and water. The electrodes were then washed in 0.1 M HCl for 10-15 min while the solution was stirred followed by ultrasonication in 0.1 M

HCl for 8-10 s, and subsequently washed with water. The electrodes were then washed in ethanol for 15-20 min with stirring, followed by water. After that, the electrodes were polished with 1 μM and 0.05 μm diamond and alumina polishing suspensions, respectively, ultrasonicated and washed with water. The electrodes were examined by cycling between -1.2 and 1.2 V. Before immobilization the electrodes were freshly polished as described in Section 2.2.

2.4. Devices and measurements.

All electrochemical measurements were performed using an Autolab potentiostat (PGGSTAT-302) controlled by Nova 2.1 software. The 0.1 M PBS solution was used as a supporting electrolyte in a three-electrode cell configuration. The Pt coil counter electrode and a double junction Ag/AgCl reference electrode, Ag | AgCl | KCl 3 M::0.5 M KCl, (Metrohm, Switzerland), were used. Electroactive surface coverage of the porphyrins on the GCE was found using the following formula [47]: $\Gamma = A/nFA\upsilon$, where Γ is the surface coverage of a porphyrin on the GCE surface, A is the surface area of an electrode, *A* is the redox peak area, n is the number of electrons transferred (n=1), and F is the Faraday constant. Unless otherwise state, the measurements were performed at a physiological pH of 7.4. The experiments with glucose oxidase were performed at pH 7.0. For measurements in deoxygenated conditions, the solutions were deaerated by bubbling Ar gas for 15 min prior to the electrochemical measurements and a stream of argon was passed over the solutions during the experiments. Unless otherwise stated the measurements were performed at ambient conditions.

All spectrophotometric measurements were performed using a PerkinElmer Lambda 900 spectrometer. The scanning electron microscopy (SEM) images were obtained using a MagellanTM XHR SEM microscope.

3. Results and discussion.

3.1. Immobilization of manganese and iron porphyrin complexes on GCEs.

In a previous study, the higher electrocatalytic activity of manganese porphyrin complexes with positively charged electron-withdrawing N-methyl-4-pyridyl *meso*-substituents of the macrocycle in the biomimetic oxygen and hydrogen peroxide reduction reactions in solutions was demonstrated [41] (additional information is provided in section S1

and Figure S1 in the supporting information). In the present study, the immobilization and hydrogen peroxide sensing properties of the porphyrin complexes with positively charged substituents of the macrocycle, MnTMPyP and FeTMPyP as well as MnTPP and FeTPP, Fig. 1, were studied and compared. Figure 2a shows cyclic voltammograms of the immobilized MnTMPyP in the deoxygenated buffer solutions with the electrochemical reduction and oxidation of the central metal ion, Mn(III/II), in the coordination center of the metalloporphyrin, which are important for the electrocatalytic conversion of hydrogen peroxide in subsequent experiments. In the absence of oxygen, the immobilized MnTMPyP displays a pair of redox peaks with the Mn(III)→Mn(II) electrochemical reduction at about -0.230 V and Mn(II)→Mn(III) oxidation in a reverse scan at about -0.090 V, Fig. 2a and Table 1. The redox potential values of the adsorbed porphyrin are slightly shifted in comparison with the redox potential values observed for this porphyrin complex in solutions [37, 41, 44, 45]. The variation can be explained by changing the environment and orientation of the metal ions in the metalloporphyrin complexes due to adsorption and confinement to the electrode surface, which can play the role of an axial ligand. Similar effects have been reported in other studies, suggesting a difference in the electrocatalysis by metalloporphyrins in the bulk dissolved and immobilized adsorbed states [42-45, 48-50]. However, the adsorbed porphyrin was not stable with the redox features disappearing during further electrochemical experiments. Electroactive surface coverage of MnTMPyP on the GCE was found as described in the experimental section 2.4 and amounted to $(1.7 \pm 0.4)\cdot10^{-11}$ mol cm^{-2}. This value is in a good agreement with the amount of adsorbed iron protoporphyrin IX (iron 3,7,12,17-tetramethyl-8,13-divinyl-2,18-porphinedipropionic acid complex) on various surfaces reported in [50] and adsorbed iron tetra(*o*-aminophenyl)porphyrin in [44].

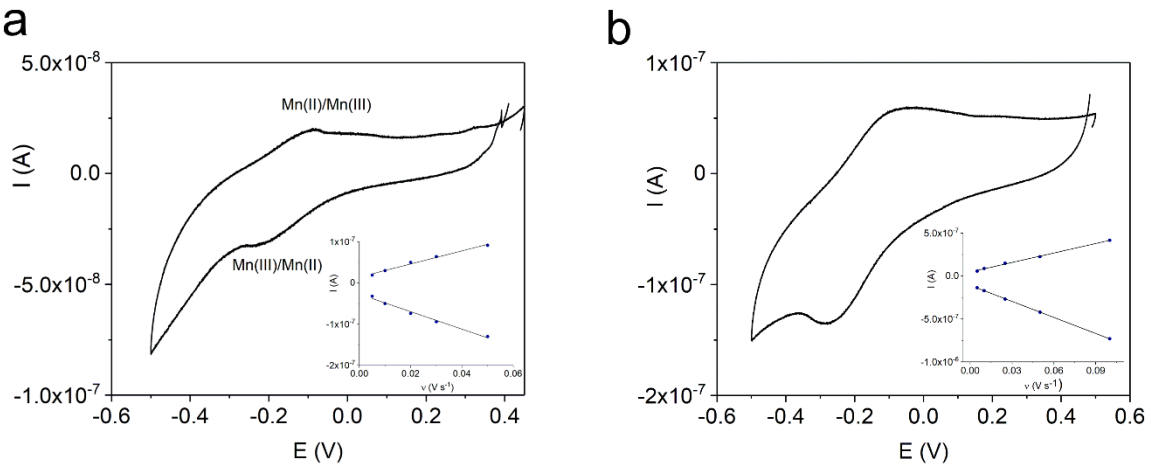

Fig. 2. CVs of the adsorbed MnTMPyP complex on a GCE recorded in a deaerated 0.1 M PBS, pH 7.4: (a) without a Nafion membrane, (b) with a Nafion(0.3 %) membrane; inserts in (a) and

(b) show dependences of the peak currents on the scan rate with the coefficients of determination [51] R^2: (a) 0.9857, 0.9829, and (b) 0.9963, 0.9998.

The experiments showed that only the MnTMPyP complex was adsorbed on the electrode surface in a quantity sufficient to observe the Mn(III/II) electrochemical redox processes reproducibly. The electrodes with FeTMPyP, MnTPP, and FeTPP did not indicate the metal ion redox reactions.

Table 1. Characterization of the metal ion redox process of the immobilized metalloporphyrin complexes and electroactive surface concentration, Γ. [1]

Electrode composition	E_{Me}^{red}, V	E_{Me}^{ox}, V	ΔE_{Me}^{redox}, V	Γ, mol cm^{-2}
MnTMPyP	-0.230	-0.090	0.140	$(1.7\pm0.4)\cdot10^{-11}$
MnTMPyP, 0.3 % Nafion	-0.269	-0.088	0.181	$(3.4\pm0.5)\cdot10^{-11}$
MnTMPyP, 1.7 % Nafion	-0.315	-0.132	0.183	$(3.2\pm0.4)\cdot10^{-11}$
FeTMPyP, 1.7 % Nafion	0.048	0.108	0.060	$(2.6\pm0.4)\cdot10^{-11}$
FeTPP, 0.3 % Nafion	0.140	0.180	0.040	$(3.5\pm0.5)\cdot10^{-11}$
FeTPP, 1.7 % Nafion	0.060	0.114	0.058	$(2.2\pm0.4)\cdot10^{-11}$

[1] adsorbed Fe(III)TPP, Fe(III)TMPyP without a Nafion membrane, and adsorbed Fe(III)TMPyP with a Nafion(0.3 %) membrane could not be detected within the conditions of the experiments, adsorption of Mn(III)TPP did not give positive results, n=3.

Different behavior of the metalloporphyrin complexes in the adsorption experiments might be also explained by different interaction with the glassy carbon surface. This was confirmed by the SEM experiments of the adsorbed porphyrins on the glassy carbon plates using the same adsorption conditions as for the GC electrodes, Fig. 3. While only the MnTMPyP complex tends to form more uniform layers on the GC surface, FeTMPyP forms additionally crystals, which might be easily washed out from the surface. The FeTPP complex shows high degree of agglomeration on the GC surface, and the MnTPP complex forms agglomerated thick layers, which probably impedes the observation of the electron transfer reaction in the latter case. Similar results were also obtained on the silicon oxide surfaces (not shown here).

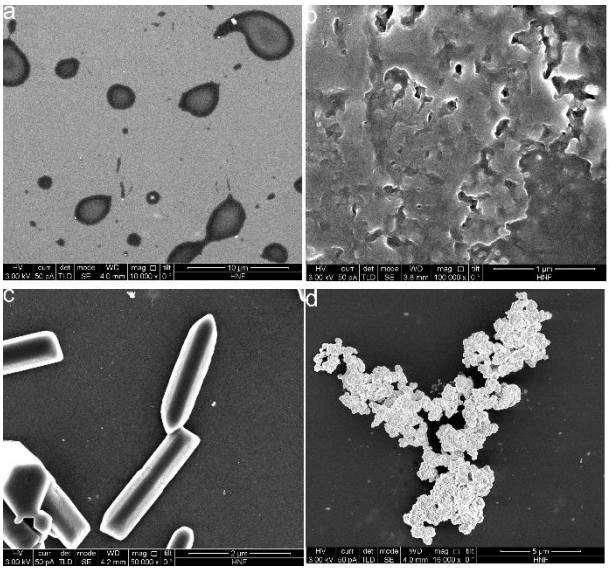

Fig. 3. SEM images of the details of the porphyrin complexes adsorbed on the GC surfaces: a - MnTMPyP, b - MnTPP, c - FeTMPyP, and d - FeTPP.

In the next series of experiments, a perfluorinated ionomer Nafion membrane was used to obtain better stability of the immobilized porphyrin complexes. Nafion is employed in electrochemical sensors and biosensors to achieve improved stability and selectivity. Nafion membranes reject negatively charged anionic interferents (e.g., ascorbic acid, AA, and uric acid, UA) and bulky interfering compounds due to the presence of negatively charged sulfonate groups and the small channel size in the nm range, respectively. The results of these experiments are presented and discussed in Section S2, Figures 2b, S2, S3, and Table 1.

Table 1 summarizes the electrochemical characterization of the adsorbed porphyrins. The surface concentration of the electroactive porphyrin complex was typically about $2 \cdot 10^{-11}$ to $3 \cdot 10^{-11}$ mol cm^{-2}. It was possible to achieve a surface concentration of the electroactive porphyrin complex of up to about 10^{-10} mol cm^{-2} using the Nafion membrane. However, the higher surface concentration resulted in wide redox peak separation or the appearance of a second reduction peak. This can be explained by a non-uniform positioning of the porphyrin molecules on the GCE surface with different distances and orientation, especially at a higher surface coverage. Larger amounts of porphyrins deposited on the electrode surface by drop casting additionally resulted in poor mechanical properties of the subsequently deposited Nafion membrane and were not employed in further experiments. Moreover, it was found that only the outmost layers of the multilayer deposited metallomacrocycles on the electrode surfaces were electrocatalytically active in the electrochemical processes [42], which also supported the use of the lower surface concentrations stated above. The diagnostic plots of the

peak current *vs*. scan rate were linear indicating the surface-confined redox processes, as expected for the adsorbed redox species, Figs. 2, S2, and S3.

The adsorption of porphyrins on the GCE was also performed from the DMF-water mixtures to achieve higher concentrations of porphyrin complexes in the solutions for the adsorption. However, the amount of immobilized porphyrin complexes was much lower in comparison with immobilization from the DMF solutions, probably due to the less favorable interactions of the complexes with the GCE surface in this case.

The quality of the Nafion coating was also examined by cyclovoltammetry. Figures 4 (ambient conditions) and S4 (deaerated solutions) show that no redox processes of the negatively charged anion hexacyanoferrate, $[Fe(CN)_6]^{3-/4-}$, are observed on the electrodes coated with the Nafion membrane in comparison with a bare GCE.

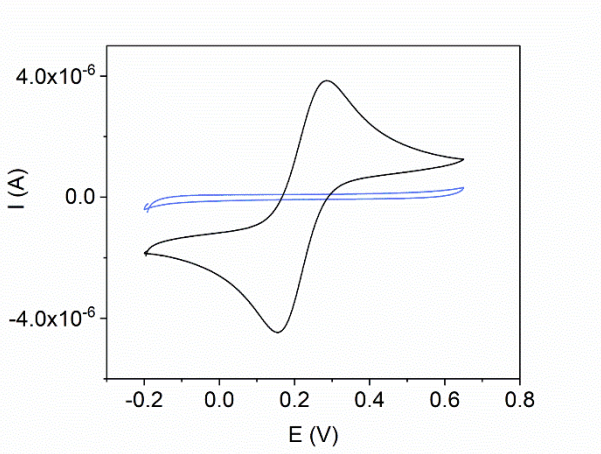

Fig. 4. Cyclic voltammograms of $5 \cdot 10^{-4}$ M potassium hexacyanoferrate(III) solution on a bare GCE (black line) and GCE/MnTMPyP/Nafion(0.3%) electrode (blue line). Other conditions: 0.1 M PBS, pH 7.4, scan rate 0.05 V s^{-1}.

Thus, in comparison with other porphyrins tested, the MnTMPyP complex is easily adsorbed on a GCE surface and can be immobilized on a GCE with a lower amount of Nafion, while for the FeTMPyP complex a higher amount of Nafion is required to achieve a stable and reproducibly modified electrode. The latter was found to be in agreement with the observations of Su et al. [45], where the FeTMPyP complex was easily washed off with water from the carbon surfaces.

3.2. Influence of amino acids.

Since natural enzyme catalysts with heme metal active centers involve proximal and distal axial amino acids in biocatalytic reactions [39, 52, 53], we performed a series of

experiments where amino acids were co-adsorbed with porphyrin complexes on a GCE using a molar ratio of metalloporphyrin:amino acid of 1:1 and 1:2. In enzymatic catalysis, the axially ligated amino acids may act as a proton source for the formation of water molecules or as a base in the deprotonation step of hydrogen peroxide [53]. It was previously shown that the co-adsorption of histidine with iron porphyrin complex improved performance of a biomimetic sensor for the determination of phenolic compounds [52]. We examined the co-adsorption of tyrosine and histidine amino acids, since these amino acids mostly occur in the heme metal active centers of enzymes playing a significant role in enzymatic reactions [39, 53, 54]. In particular, horseradish peroxidase oxidizes such substrates as aromatic amines and phenols reducing hydrogen peroxide and involves histidine as a proximal ligand of a heme iron, while catalase involves tyrosine as a proximal ligand catalyzing the disproportionation of hydrogen peroxide to water and oxygen. In the case of the synthetic metalloporphyrin complexes, it was shown that proximal ligands bearing oxygen groups reduced the oxygenase activity of the metalloporphyrins in comparison with the complexes with nitrogen-containing axial ligands.

In the case of iron porphyrin complexes, the presence of the tyrosine and histidine amino acids in adsorption solutions resulted in electrodes with no or extremely weak redox features of the porphyrins under the conditions of experiments. Only immobilization of MnTMPyP with tyrosine resulted in electrodes with electrochemical features of the MnP complex. However, we observed that in the case of the co-adsorption of the manganese porphyrin complexes with tyrosine and histidine, redox peaks in a positive voltage range at about 0.116 V emerged reproducibly, as shown in Fig. 5 (marked with arrows). We assume that these peaks may originate from changing the coordination of the manganese ions due to the presence of such ideal coordinating ligands as histidine and tyrosine [55, 56]. Therefore, electrochemical experiments were performed with the corresponding amino acids and manganese chloride. While cyclic voltammograms of histidine did not reveal significant electrochemical redox processes in a positive potential range, manganese chloride demonstrated reduction and oxidation peak currents in the studied potential range at 0.08 V and 0.380 V, respectively, Fig. 5 b. In the case of tyrosine, an irreversible oxidation current can be observed starting, however, at higher potential values of about 0.5 V, which is explained by its oxidation on a GCE [57, 58]. This confirms our hypothesis that the origin of the redox processes in a positive voltage range is not in the redox processes of the amino acids themselves, but is due to variation of the redox potentials of the adsorbed manganese complex because of partly changing the coordination of the manganese ions due to the presence of histidine and tyrosine ligands. The same phenomenon can also explain a poor adsorption of the porphyrin complexes on the GCE

surface in the presence of amino acids, where the amino acids may compete with the GCE surface for the axial ligand sites and should be generally taken into account when co-immobilizing various sensor components.

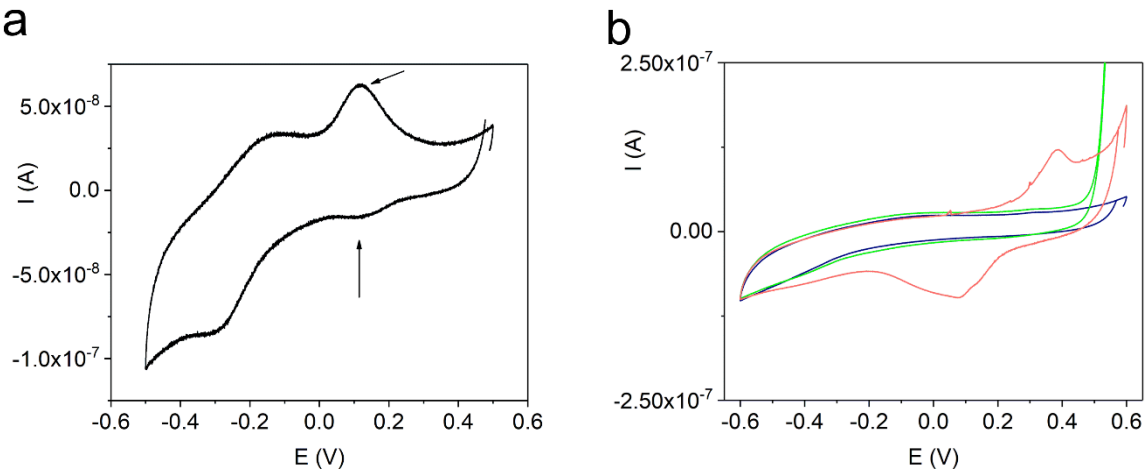

Fig. 5. Cyclic voltammograms of the GCE: (a) MnTMPyP co-adsorbed with tyrosine on the GCE, GCE/MnTMPyP+Tyr/0.3 % Nafion, in a deaerated 0.1 M PBS, pH 7.4, arrows mark a new pair of redox peaks, (b) amino acids histidine (blue line) and tyrosine (green line) in a deaerated 0.1 M PBS, pH 7.4, and $MnCl_2$ (red line) in a deaerated 0.1 M KNO_3, scan rate 0.005 V s^{-1},

3.3. Hydrogen peroxide sensor properties.

The electrodes which demonstrated the $M^{III/II}$ electrochemical reduction and oxidation processes of the metalloporphyrin complexes adsorbed on the GCEs were further tested for their hydrogen peroxide sensing properties at ambient conditions. Along with iron porphyrins, manganese porphyrins have been proposed for enzyme mimetics, having the additional advantage of not participating in the Fenton reaction in biological systems, which leads to considerable interest in their sensor properties for ROS detection [9]. We previously performed an investigation of a series of manganese porphyrins in the electrocatalytic reduction of hydrogen peroxide in aqueous solutions [41] (additional supporting information is also provided in Section 1 and Fig. S1). In the presence of oxygen and hydrogen peroxide, electrochemical reduction and oxidation processes of the central metal ion, $Me^{III/II}P$, were not observed in cyclic voltammograms, while the cathodic currents increased, Fig. 6a,b. These characteristics are explained by the electrocatalytic effect of the manganese porphyrins in the oxygen and hydrogen peroxide reduction processes according to a number of proposed biomimetic mechanisms [41]. Electrocatalytic reduction of oxygen and hydrogen peroxide starts at potentials close to the potential of the Me(III/II) redox couple, Fig. S1. Accordingly,

the electrochemically generated metal-reduced forms of the manganese porphyrins, Mn(II)P, are involved in the reaction with oxygen and hydrogen peroxide oxidants and are regenerated due to electrocatalyst redox cycling [37, 41, 59], Scheme 1. Scheme 1 describes the biomimetic response of the sensor based on MnTMPyP, while for the iron porphyrins a catalytic reaction sequence has been discussed in detail [31]. It is assumed that the reaction proceeds via similar metal-oxo intermediates [39].

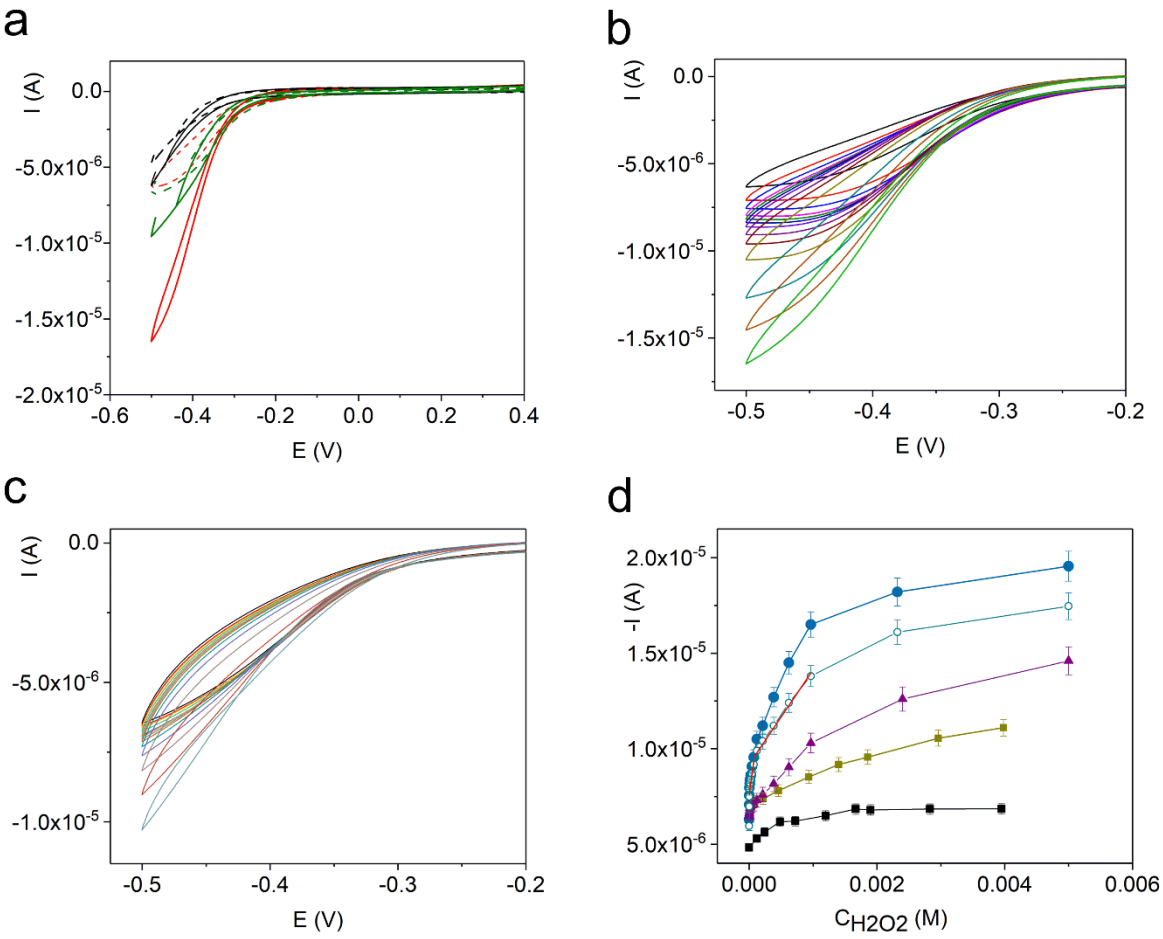

Fig. 6. Cyclic voltammograms in 0.1 M PBS, pH 7.4: (a) a bare GCE (black lines), GCE/FeTMPyP/Nafion(1.7 %) (green lines), and GCE/MnTMPyP/Nafion(0.3%) (red lines) with 0 M (dashed lines) and $1 \cdot 10^{-3}$ M H_2O_2 (solid lines), (b) GCE/MnTMPyP/Nafion(0.3%) with H_2O_2 from 0 to $1 \cdot 10^{-3}$ M; (c) GCE/MnTMPyP+Tyr/Nafion(0.3%) with H_2O_2 from 0 to $1 \cdot 10^{-3}$ M; (d) dependence of the current on the concentration of hydrogen peroxide of a bare GCE (black) at -0.5 V, GCE/FeTMPyP/Nafion(1.7%) (violet) at -0.5 V, GCE/MnTMPyP+Tyr/Nafion(0.3%) (dark yellow) at -0.5 V, and GCE/MnTMPyP/Nafion(0.3%) at -0.5 V (blue) and -0.45 V (cyan). Other conditions: scan rate 0.05 V s^{-1}, the measurements were performed at ambient conditions. Error bar represent the confidence limits (p = 0.95, n = 5) at each concentration point.

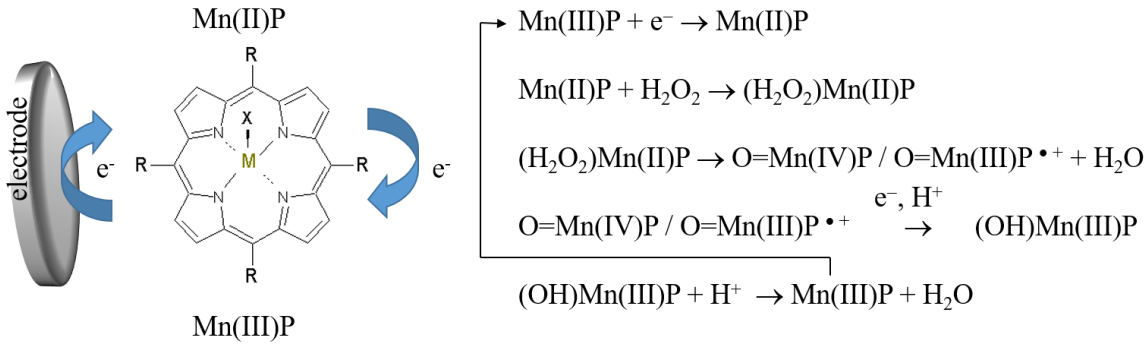

Scheme 1. Scheme of the electrocatalytic reduction of hydrogen peroxide on the electrode modified by a manganese porphyrin complex.

Of all the compositions examined, electrodes with the immobilized Fe(III)TMPyP and Mn(III)TMPyP complexes with Nafion membranes deposited from the 1.7 % and 0.3 % solutions, respectively, had the highest sensitivity to hydrogen peroxide, Fig. 6a and d. The GCE/MnTMPyP/Nafion(0.3%) electrodes demonstrated significantly better performance with higher sensitivity and sensitivity in a lower concentration range of hydrogen peroxide than bare GCE and GCE with the adsorbed Fe(III)TMPyP, as can be seen from Figure 6a,d. The observed lower electrocatalytic activity of FeTMPyP in hydrogen peroxide electroreduction is in agreement with a previously discussed preferable two-electron reduction of oxygen to hydrogen peroxide by Fe porphyrins, but not of hydrogen peroxide to water [60]. Our results agree with the higher peroxidase-like activity of the Mn porphyrin complex in comparison with Fe-, Co-, Cu-, Zn-, and metal-free porphyrins immobilized on ion-exchange resin [40]. Co-adsorption of MnTMPyP with tyrosine did not improve sensor performance in comparison with the GCE/MnTMPyP sensor, Fig. 6c,d. The response of the biomimetic sensor at the detection potential of -0.45 V can be approximated by a linear range of $6 \cdot 10^{-7}$ M to $4 \cdot 10^{-5}$ M with a sensitivity found from the linear regression equation of 1.8 A M^{-1} cm^{-2} ($y=6.71 \cdot 10^{-6} + 0.126x$, $R^2=0.6202$) and $4 \cdot 10^{-5}$ M to $1 \cdot 10^{-3}$ M with a sensitivity of 0.071 A M^{-1} cm^{-2} ($y=9.19 \cdot 10^{-6} + 4.94 \cdot 10^{-3}x$, $R^2=0.9793$). The dependence of the reduction current on the hydrogen peroxide concentration is also observed at higher concentrations of hydrogen peroxide, but with lower sensitivity, Fig. 6d. The detection limit was found based on the standard deviation of the response and the slope according to the ICH recommendations [61] as 3.3·S/b, where S is the standard deviation of the blank sample measurements and b is the slope of the calibration curve in a low concentration range. The detection limit was as low as $5 \cdot 10^{-7}$ M H_2O_2. According to [61], the low limit of quantitation, LLOQ, was found as 10·S/b and equaled $1.5 \cdot 10^{-6}$ M H_2O_2. It

is important that hydrogen peroxide detection at the negative potential in our work can be performed in the presence of oxygen, Fig. 6, which is essential for the analytical application of the sensor [62], while some sensors can be applied only in the deoxygenated solutions. A negative detection potential is favorable for achieving higher selectivity with respect to oxidizable compounds, such as uric acid and ascorbate, since these electrochemical processes do not proceed at negative potentials [63]. Table 2 compares characteristics of the sensor with other recently reported electrochemical sensors for hydrogen peroxide detection based on the metal complexes. As one can see from the table, a number of the reported sensors allow to achieve low detection limits and reasonable sensitivities only in alkaline conditions, e.g., sensors based on metal-organic frameworks [64, 65], or in the absence of oxygen [66], which is not favorable for their practical applications. Biomimetic sensor based on the immobilized MnTMPyP complex proposed in the present work demonstrates a higher sensitivity in the low concentration range of hydrogen peroxide than other proposed sensors based on metal complexes, Table 1. The sensor is also characterized with a low detection limit and large working range in comparison with other sensors based on metal complexes reported in literature [10, 16, 64-67]. Thus, the table demonstrates that along with an easy fabrication procedure and simple storage conditions, the biomimetic electrocatalytic properties of the MnTMPyP complex facilitate excellent performance of the proposed sensor.

Previously, we found that in the presence of MnTMPyP in the solution the electrocatalytic reduction currents were higher in the presence of oxygen than in the deaerated conditions in the same concentration range of hydrogen peroxide [41]. The electrochemical response of the GCE/MnTMPyP/Nafion(0.3%) sensors was also examined in the absence of oxygen (in deaerated conditions), Fig. S5. In the case of the immobilized MnTMPyP catalyst, the electrocatalytic reduction currents were higher at ambient conditions (in the presence of oxygen), Fig. 6b, which is similar to the experiments with the MnTMPyP complex in the solution. This behavior can be explained by a number of parallel processes with participation of superoxide radical anion produced from the electrocatalytic reduction of oxygen [41] so that due to the synergy of electrocatalytic effect of MnTMPyP complex and oxygen higher reduction currents and higher sensitivity to hydrogen peroxide are observed at ambient conditions.

Selectivity of the GCE/MnTMPyP/Nafion for a number of interfering substances was studied evaluating the effect of the electroactive species on the analytical signal of the biomimetic sensors. Figure 7a demonstrates the sensor response to the consecutive addition of H_2O_2, aminobutyric, ascorbic, glutamic acids, glucose, uric acid, and dopamine. The sensor is characterized by high selectivity to the common interferents. The sensors can be easily stored

in dry condition at room temperature. Stability of the sensor response over 10 days is shown in Figure 7b. On days 7 and 10 under normal storage conditions, the sensor response to 10^{-5} M H_2O_2 retained 94 % and 91 % of the initial value, respectively. The relative standard deviation of five measurements within a day was between 4 % and 5 %. Thus, the characteristics of the sensor such as low detection limit, high selectivity, stability, and precision [61, 68] are favorable for its application.

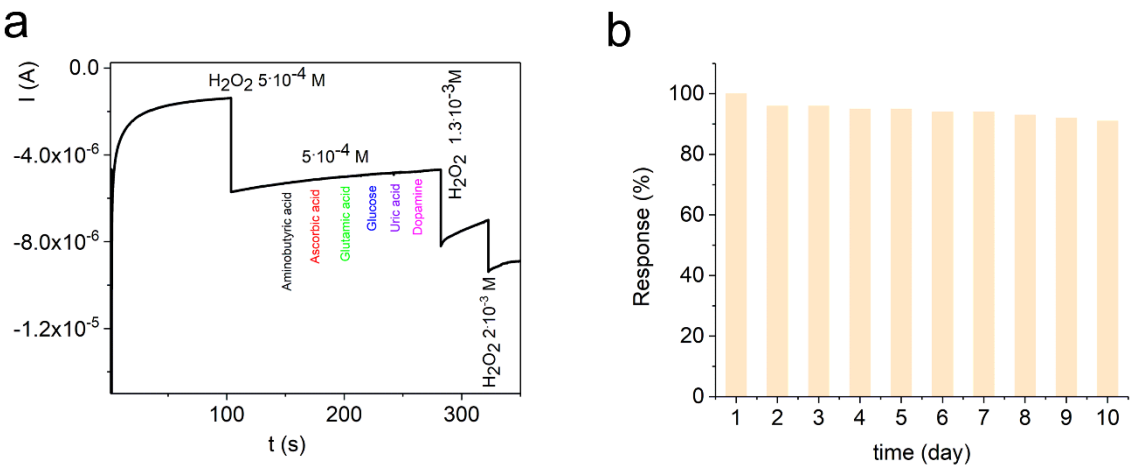

Fig. 7. (a) Selectivity studies of the GCE/MnTMPyP/Nafion(0.3 %) sensor in 0.1 M PBS, pH 7.4, applied potential is -0.45 V, (b) stability of the GCE/MnTMPyP/Nafion sensor response to 10^{-5} M H_2O_2. The measurements were performed at ambient conditions.

Table 2. Comparison of the hydrogen peroxide electrochemical sensors for hydrogen peroxide detection based on metal complexes.

Electrode	Potential, V	pH	Linear range (μm)	LOD (μM)	Sensitivity (mA mM^{-1} cm^{-2})	Ref.
GMCF/Hb/Nafion	-0.5	7.0	8 - 210	2	1.4	[25]
GCE/ZnO-GNP-HRP-Nafion	-0.3	7.0	15 - $1.1 \cdot 10^3$	9		[67]
GCE/Ni(II)MOF-CNT/Nafion	+0.5	0.1 M NaOH	10 - $51.6 \cdot 10^3$	2.1	0.12	[64]
GCE/pFeMOF-OMC/Nafion	-0.31	7.4	0.5 - 70.5, 70.5-1830.5	0.45	0.96 0.32	[30]

GCE/CoMOF/Nafion	-0.4	0.1 M NaOH	$5 - 9 \cdot 10^3$	3.76	0.083	[65]
GCE/$CoSn(OH)_6$-Nafion	-0.6	7.0, N_2-deoxygenated	4 - 400	1	0.019	[66]
Au/AuNW/HRP	-0.07	6.8	18-500	5	0.031	[10]
GCE/f-MWCNT@$Mn(bpy)_2(H_2O_2)_2$/Nafion	+0.65	7.0	20 - 200	1	-	[16]
GCE/MnTMPyP/Nafion	-0.45	7.4	0.6 - 40 40 - 1000	0.5	1.8 0.071	this work

GMCF - graphene modified carbon fiber, Hb – hemoglobin, GCE – glassy carbon electrode, MOF-metal-organic framework, GNP – gold nanoparticles, pFeMOF porphyrinic iron metal organic framework; OMC – ordered mesoporous carbon, AuNW - gold nanowires, MWCNT – multi walled carbon nanotubes

The pH dependence of the sensor response is shown in Figure 8. It is interesting that this dependence differs from the pH dependence of the electrocatalytic properties of the MnTMPyP complex in hydrogen peroxide reduction the solutions [41]. In the latter case, the electrocatalytic properties were higher in acidic and alkaline solutions. In alkaline solutions, hydrogen peroxide starts to partially dissociate (pK_a 11.6). As a result, the negatively charged HO_2^- anions do not reach the porphyrin active layer due to the negative ion repelling properties of the Nafion membrane. Thus, the apparent concentration of the hydrogen peroxide is diminished, which can explain the lower sensor sensitivity. A lower sensitivity of the sensor in acidic solution might be influenced by a high proton conductivity of the Nafion membrane.

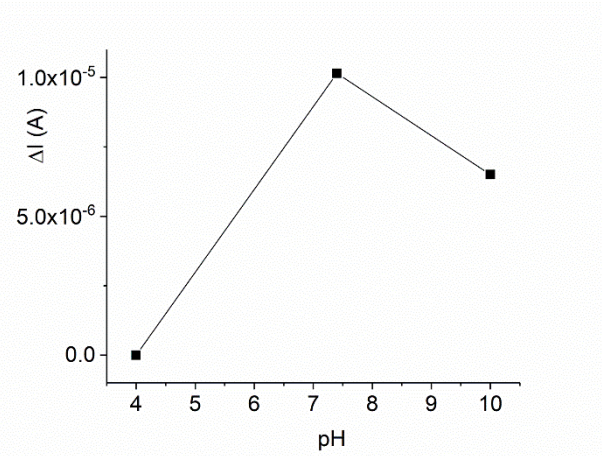

Fig. 8. Sensor response to $9.6 \cdot 10^{-4}$ M M H_2O_2 in buffer solutions with pH 4, 7.4, and 10.

3.4. Analytical application of the hydrogen peroxide sensors based on the MnTMPyP complex.

An analytical application of the biomimetic sensors based on the electrocatalytic reduction of hydrogen peroxide with the immobilized MnTMPyP complex and the influence of the biological matrix on the sensor response have been explored for the detection of hydrogen peroxide and glucose in biological samples. µM concentration ranges of hydrogen peroxide in biological systems have been reported such as hydrogen peroxide concentrations in human blood from a possible low of 0.25 µM to a probable normal range of 1-5 µM, and a higher range of 30-50 µM in diseased states or inflammation [69], as well as endogenous H_2O_2 levels of 1-50 µM in brain [70]. Figure 9 shows a sensor response in the heat inactivated human serum diluted with 0.1 M PBS (pH 7.4) 1:2 v/v to the exogenous hydrogen peroxide. The sensitivity of the sensor in the human serum diluted with PBS was found from the linear regression of the experimental data and decreased slightly in comparison with that in PBS due to the influence of the biological matrix. The sensitivity was 0.43 A M^{-1} cm^{-2} (R^2=0.7839) in the lower concentration range of $6 \cdot 10^{-7}$ to $4.5 \cdot 10^{-6}$ and 0.027 A M^{-1} cm^{-2} (R^2=0.9927) in the higher concentration range of $4.5 \cdot 10^{-6}$ to $1.7 \cdot 10^{-3}$ M. The sensitivity of the sensor in the human serum diluted with PBS was found to be higher than in the human serum diluted with a borate buffer of pH 10, which is in agreement with Fig. 8.

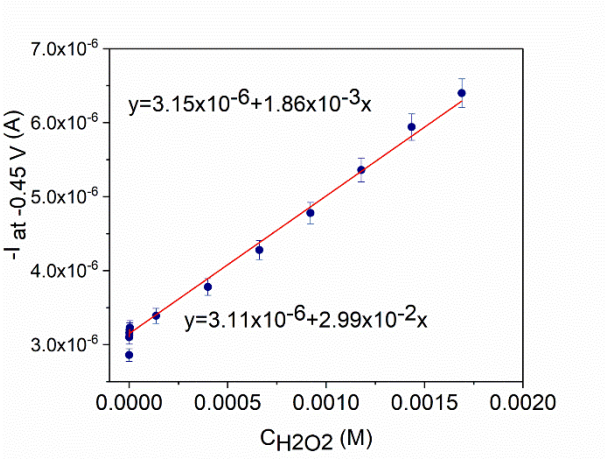

Fig. 9. Dependence of the reduction current on the exogenous hydrogen peroxide of the GCE/MnTMPyP/Nafion(0.3 %) sensor in the human serum diluted with 0.1 M PBS (pH 7.4) 1:2 v/v at -0.45 V, with the linear regression equations and lines, scan rate 0.05 V s^{-1}, the measurements were performed at ambient conditions.

The feasibility of the sensor for the practical analysis is further demonstrated in Table 2, which presents the results of the determination of the hydrogen peroxide in human serum samples by a spike procedure in terms of apparent recovery, R_a, [68, 71]. Known amounts of hydrogen peroxide were added to the diluted serum samples and the concentration of hydrogen peroxide was determined using a calibration graph, Table 2. The values of bias [68] and apparent percent recovery [68] by the assay of known added amount of hydrogen peroxide in the sample which characterize the accuracy [61] indicate that the sensor can be used for the determination of hydrogen peroxide in biological samples.

Table 3. Analysis of hydrogen peroxide in human serum samples using the biomimetic sensor.[a]

Hydrogen peroxide added, μM	Hydrogen peroxide concentration found by the sensor, μM[b]	Bias, %	R_a (n=3), %
3.2	3.3±0.2	3.1	103
7.8	7.6±0.4	2.6	97
16	15.6±0.6	2.5	98

[a] Concentration of hydrogen peroxide in the heat inactivated human serum sample was found to be below 1 μM by spectrophotometric determination using horseradish peroxidase-coupled oxidation of 4-aminoantipyrine and phenol as donor substrates according to procedure [72], which is in accordance with the study of [73] for the standard serum preparation.

[b] - confidence intervals are found for n=3 and confidence level p=0.95 [68, 74].

3.5. Glucose sensing properties of the sensor based on the MnTMPyP complex.

The signal transducer properties of the modified GCE/MnTMPyP-GOx-Nafion electrode were tested for glucose sensing. Glucose oxidase (beta-D-glucose: oxygen 1-oxidoreductase, EC 1.1.3.4) selectively catalyzes the two-electron, two-proton oxidation of glucose to gluconolactone by molecular oxygen with the hydrogen peroxide product of the oxygen reduction according to the reaction:

$$\text{glucose} + O_2 \rightarrow \text{gluconolactone} + H_2O_2$$

The GCE/MnTMPyP-GOx-Nafion sensors were prepared as described in Sections 2.2. and S3. When glucose was introduced into the solution with the GCE/MnTMPyP-GOx-Nafion sensor, a reproducible decrease of the reduction currents was observed for the electrodes prepared using both immobilization procedures of the glucose oxidase, as well as for the

electrodes, where no MnTMPyP complex was co-immobilized (used for comparison), Fig. 10. The decrease of the reduction current is due to oxygen consumption in the process of glucose oxidation catalyzed by GOx. This behavior can probably be explained by a number of factors such as particular orientation of the enzyme favoring consumption and depletion of oxygen in the enzymatic reaction of glucose oxidation within the Nafion membrane and near the electrode surface with the immobilized porphyrin. Additionally, diffusion and removal of hydrogen peroxide from the electrode surface to the solution may contribute. It is worth noting that a diminished response of the glucose sensor under depletion of oxygen has been previously reported [46]. In this case, the electrocatalytic activity of MnTMPyP in oxygen reduction [41], section S1 and Fig. S1, allows a high sensitivity of the sensor to be achieved, Fig. 10. Therefore, it can be concluded that the mechanism of the sensor response with the immobilized MnTMPyP complex corresponds to the mechanism of the first generation of enzyme sensors with O_2 as a natural mediator, where oxygen consumption by the enzyme-catalyzed reaction is monitored as an analytical signal.

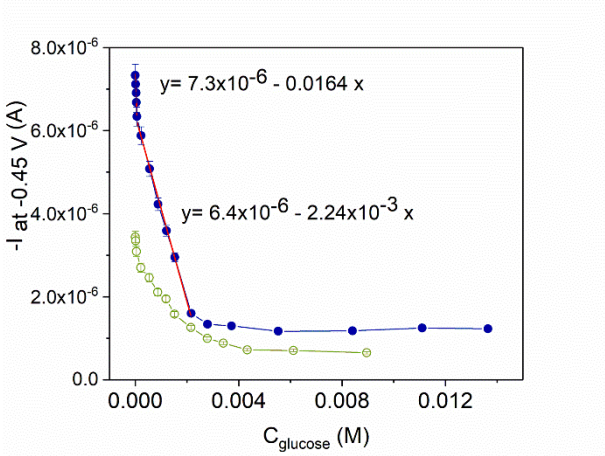

Fig. 10. Dependence of the current on the concentration of glucose in 0.1 M PBS, pH 7.0, at -0.45 V for the GCE/MnTMPyP-GluOx-Nafion sensor prepared by method 1 (blue symbols) with the linear regression equations and lines (in red), R^2 is 0.9908 and 0.9962 for the lower and higher glucose concentration ranges, respectively, and GCE/GluOx/Nafion electrode (green symbols). Other conditions: scan rate 0.05 V s^{-1}, n=3, solutions were stirred between measurements to prevent formation of the oxygen depletion layer at the electrode surface.

Figure 10 demonstrates that due to the electrocatalytic properties of the electrode with the immobilized MnTMPyP in the oxygen reduction reaction, this sensor has a high sensitivity to glucose of 0.234 A M^{-1} cm^{-2} (0.9908) in a lower glucose concentration range of 0.01 mM - 0.1 mM and 0.032 A M^{-1} cm^{-2} (0.9962) in a higher glucose concentration range of 0.1 mM - 2

mM and stability, Fig. S6. RSD% of five measurements within one day was about 4 %. The detection limit and LLOQ were found as described in section 3.3 [61] and equaled 0.008 mM and 0.024 mM glucose, respectively. Table 4 shows the results of the determination of glucose in the human serum samples using a spike procedure in terms of bias and apparent recovery [68, 71]. The accuracy reported as the percent bias and apparent recovery by the assay of known amount of glucose in the sample [61] indicate that the sensor can be successfully used for the analysis of the glucose level in serum samples. Moreover, the sensor does not relay on the use of a mediator that should dissolve in the sample and it works at neutral pH at potentials far from the oxidizing potentials of interferences, while many comparable sensors are working in alkaline media, Table S1. These characteristics are advantageous for using the proposed sensor in the analysis of glucose in biological samples and development of point-of-care devices.

Table 4. Analysis of glucose in serum samples using the biomimetic sensor based on the co-immobilized Mn porphyrin and glucose oxidase.[a,b]

Glucose in a diluted serum sample, mM [c]	Glucose concentration added, mM	Glucose concentration found, mM[d]	Bias, %	R_a (n=3), %
0.52	0.1	0.51 ± 0.03	3.8	96
0.52	0.4	0.94 ± 0.04	2.2	102
0.52	0.8	1.29 ± 0.05	2.3	98
0.52	2	2.44 ± 0.11	3.2	97

[a] Normal blood glucose level: 3.9 - 6.1 mM, the concentration range for the commercial blood glucose monitors is 0.5 - 15 mM.
[b] Serum was diluted 1:9 v/v with 0.1 M PBS, pH 7.0.
[c] Determined independently by the spectrophotometric method as described for Table 3.
[d] Confidence intervals are found for n=3 and confidence level p=0.95 [68, 74].

Conclusions.

Non-enzymatic biomimetic sensors for hydrogen peroxide based on a series of immobilized porphyrin complexes of iron and manganese were prepared and investigated. The influence of the *meso*-substituents of the macroheterocyclic porphyrin ligand, composition of the adsorption solution, Nafion membrane, and amino acids on the properties of the sensors were studied. The MnTMPyP complex achieved the best sensor performance for the determination of hydrogen peroxide in the presence of oxygen with a low detection limit of

$5 \cdot 10^{-7}$ M H_2O_2, high sensitivity to hydrogen peroxide of up to 1.8 A M^{-1} cm^{-2} in a low concentration range, and high selectivity, which makes it possible to use it for the analysis of biological media. It was shown that the sensors can be used for the determination of hydrogen peroxide in human serum. Furthermore, the signal transducer properties of the adsorbed MnTMPyP for oxidase-based biosensors were investigated and glucose in human serum samples was determined. Along with a simple fabrication procedure and robustness of the sensor, the biomimetic electrocatalytic properties of the MnTMPyP complex in hydrogen peroxide and oxygen reduction allowed excellent performance of the proposed electrochemical sensors to be achieved for hydrogen peroxide and glucose determination in biological media, emphasizing a bright perspective of the biomimetic electrocatalytic metalloporphyrin complexes in healthcare and bioenergetics.

Acknowledgements: Dr. R. Peng acknowledges the Helmholtz-OCPC Postdoc Program (20181032) for the financial support. The authors thank E. Brauweiller-Reuters for the SEM studies.

References.

[1] C. Jacob, P.G. Winyard, (eds.), Redox signaling and regulation in biology and medicine, Weinheim: Wiley-VCH; 2009.
[2] S. Parvez, M.J.C. Long, J.R. Poganik, Y. Aye, Redox Signaling by Reactive Electrophiles and Oxidants, Chem Rev, 118(2018) 8798-888.
[3] A. Prasad, A. Kumar, M. Suzuki, H. Kikuchi, T. Sugai, M. Kobayashi, et al., Detection of hydrogen peroxide in Photosystem II (PSII) using catalytic amperometric biosensor, Frontiers in Plant Science, 6(2015).
[4] B. Yang, Y. Chen, J. Shi, Reactive Oxygen Species (ROS)-Based Nanomedicine, Chem Rev, 119(2019) 4881-985.
[5] W. Sun, Q. Sun, Bioinspired Manganese and Iron Complexes for Enantioselective Oxidation Reactions: Ligand Design, Catalytic Activity, and Beyond, Accounts of Chemical Research, 52(2019) 2370-81.
[6] D. Vione, V. Maurino, C. Minero, E. Pelizzetti, The atmospheric chemistry of hydrogen peroxide: a review., Ann Chim, 93(2003) 477-88.
[7] J.M. Anglada, M. Martins-Costa, J.S. Francisco, M.F. Ruiz-López, Interconnection of Reactive Oxygen Species Chemistry across the Interfaces of Atmospheric, Environmental, and Biological Processes, Accounts of Chemical Research, 48(2015) 575-83.
[8] J.C. Barona-Castaño, C.C. Carmona-Vargas, T.J. Brocksom, K.T. De Oliveira, Porphyrins as catalysts in scalable organic reactions, Molecules, 21(2016) 310.
[9] C. Calas-Blanchard, G. Catanante, T. Noguer, Electrochemical Sensor and Biosensor Strategies for ROS/RNS Detection in Biological Systems, Electroanalysis, 26(2014) 1277-86.
[10] E. Koposova, G. Shumilova, Y. Ermolenko, A. Kisner, A. Offenhaeusser, Y. Mourzina, Direct electrochemistry of cyt c and hydrogen peroxide biosensing on oleylamine- and citrate-stabilized gold nanostructures, Sensors and Actuators B-Chemical, 207(2015) 1045-52.

[11] H. Guan, Y. Zhao, J. Zhang, Y. Liu, S. Yuan, B. Zhang, Uniformly dispersed PtNi alloy nanoparticles in porous N-doped carbon nanofibers with high selectivity and stability for hydrogen peroxide detection, Sensors and Actuators B: Chemical, 261(2018) 354-63.
[12] E. Koposova, X. Liu, A. Kisner, Y. Ermolenko, G. Shumilova, A. Offenhaeusser, et al., Bioelectrochemical systems with oleylamine-stabilized gold nanostructures and horseradish peroxidase for hydrogen peroxide sensor, Biosensors & Bioelectronics, 57(2014) 54-8.
[13] H. Li, H. Zhao, H. He, L. Shi, X. Cai, M. Lan, Pt-Pd bimetallic nanocoral modified carbon fiber microelectrode as a sensitive hydrogen peroxide sensor for cellular detection, Sensors and Actuators B: Chemical, 260(2018) 174-82.
[14] K.G. Nikolaev, Y.E. Ermolenko, A. Offenhausser, S.S. Ermakov, Y.G. Mourzina, Multisensor Systems by Electrochemical Nanowire Assembly for the Analysis of Aqueous Solutions, Frontiers in Chemistry, 6(2018).
[15] K.G. Nikolaev, V. Maybeck, E. Neumann, S.S. Ermakov, Y.E. Ermolenko, A. Offenhausser, et al., Bimetallic nanowire sensors for extracellular electrochemical hydrogen peroxide detection in HL-1 cell culture, Journal of Solid State Electrochemistry, 22(2018) 1023-35.
[16] N. Saravanan, P. Mayuri, S.-T. Huang, A.S. Kumar, In-situ electrochemical immobilization of [Mn(bpy)2(H2O)2]2+ complex on MWCNT modified electrode and its electrocatalytic H2O2 oxidation and reduction reactions: A Mn-Pseudocatalase enzyme bio-mimicking electron-transfer functional model, Journal of Electroanalytical Chemistry, 812(2018) 10-21.
[17] M.A. Komkova, A. Pasquarelli, E.A. Andreev, A.A. Galushin, A.A. Karyakin, Prussian Blue modified boron-doped diamond interfaces for advanced H2O2 electrochemical sensors, Electrochimica Acta, 339(2020) 135924.
[18] C. Cui, Q. Wang, Q. Liu, X. Deng, T. Liu, D. Li, et al., Porphyrin-based porous organic framework: An efficient and stable peroxidase-mimicking nanozyme for detection of H2O2 and evaluation of antioxidant, Sensors and Actuators B: Chemical, 277(2018) 86-94.
[19] X. Liu, H. Li, F. Wang, S. Zhu, Y. Wang, G. Xu, Functionalized single-walled carbon nanohorns for electrochemical biosensing, Biosensors and Bioelectronics, 25(2010) 2194-9.
[20] M.J. Schöning, A.E. Poghossian, Label-Free Biosensing. Advanced Materials, Devices and Applications: Springer; 2018.
[21] Y. Liu, H. Li, S. Gong, Y. Chen, R. Xie, Q. Wu, et al., A novel non-enzymatic electrochemical biosensor based on the nanohybrid of bimetallic PdCu nanoparticles/carbon black for highly sensitive detection of H2O2 released from living cells, Sensors and Actuators B: Chemical, 290(2019) 249-57.
[22] D. Rojas, F. Della Pelle, M. Del Carlo, M. d'Angelo, R. Dominguez-Benot, A. Cimini, et al., Electrodeposited Prussian Blue on carbon black modified disposable electrodes for direct enzyme-free H2O2 sensing in a Parkinson's disease in vitro model, Sensors and Actuators B-Chemical, 275(2018) 402-8.
[23] Y. Li, M. Xie, X. Zhang, Q. Liu, D. Lin, C. Xu, et al., Co-MOF nanosheet array: A high-performance electrochemical sensor for non-enzymatic glucose detection, Sensors and Actuators B: Chemical, 278(2019) 126-32.
[24] K. Nikolaev, S. Ermakov, Y. Ermolenko, E. Averyaskina, A. Offenhausser, Y. Mourzina, A novel bioelectrochemical interface based on in situ synthesis of gold nanostructures on electrode surfaces and surface activation by Meerwein's salt. A bioelectrochemical sensor for glucose determination, Bioelectrochemistry, 105(2015) 34-43.
[25] J. Bai, L. Wu, X. Wang, H.-M. Zhang, Hemoglobin-graphene modified carbon fiber microelectrode for direct electrochemistry and electrochemical H2O2 sensing, Electrochimica Acta, 185(2015) 142-7.
[26] L. Lvova, C. Di Natale, R. Paolesse, Porphyrin-based chemical sensors and multisensor arrays operating in the liquid phase, Sensors and Actuators B: Chemical, 179(2013) 21-31.
[27] R. Paolesse, S. Nardis, D. Monti, M. Stefanelli, C. Di Natale, Porphyrinoids for Chemical Sensor Applications, Chemical Reviews, 117(2017) 2517-83.
[28] C.M. Maroneze, Y. Gushikem, L.T. Kubota, Applications of MN4 Macrocyclic Metal Complexes in Electroanalysis, in: J. Zagal, F. Bedioui (Eds.), Electrochemistry of N4 Macrocyclic Metal Complexes, Springer, Switzerland, 2016.

[29] T.A. Skripnikova, A.A. Starikova, G.I. Shumilova, Y.E. Ermolenko, A.A. Pendin, Y.G. Mourzina, Towards stabilization of the potential response of Mn(III) tetraphenylporphyrin-based solid-state electrodes with selectivity for salicylate ions, Journal of Solid State Electrochemistry, 21(2017) 2269-79.
[30] J. Liu, X. Bo, J. Yang, D. Yin, L. Guo, One-step synthesis of porphyrinic iron-based metal-organic framework/ordered mesoporous carbon for electrochemical detection of hydrogen peroxide in living cells, Sensors and Actuators B: Chemical, 248(2017) 207-13.
[31] S.M. Adam, G.B. Wijeratne, P.J. Rogler, D.E. Diaz, D.A. Quist, J.J. Liu, et al., Synthetic Fe/Cu complexes: toward understanding Heme-Copper Oxidase structure and function, Chemical Reviews, 118(2018) 10840-1022.
[32] P. Mineo, E. Scamporrino, E. Spina, D. Vitalini, Synthesis and characterization of copolyformals containing electron-rich or electron-poor porphyrin units in the main chain and their use as sensors, Sensors and Actuators B: Chemical, 188(2013) 1284-92.
[33] M.L. Pegis, C.F. Wise, D.J. Martin, J.M. Mayer, Oxygen reduction by homogeneous molecular catalysts and electrocatalysts, Chemical Reviews, 118(2018) 2340-91.
[34] S.M. Kuzmin, S.A. Chulovskaya, V.I. Parfenyuk, Superoxide-assisted electrochemical deposition of Mn-aminophenyl porphyrins: Process characteristics and properties of the films, Electrochimica Acta, 292(2018) 256-67.
[35] T. Ohse, S. Nagaoka, Y. Arakawa, H. Kawakami, K. Nakamura, Cell death by reactive oxygen species generated from water-soluble cationic metalloporphyrins as superoxide dismutase mimics, J Inorg Biochem, 85(2001) 201-8.
[36] I. Batinić-Haberle, J.S. Rebouças, I. Spasojević, Superoxide dismutase mimics: chemistry, pharmacology, and therapeutic potential, Antioxid Redox Signal, 13(2010) 877-918.
[37] N. Kobayashi, H. Saiki, T. Osa, Catalytic electroreduction of molecular oxygen using [5,10,15,20-tetrakis-(1-methylpyridinium-4-yl)porphinato]manganese, Chemistry Letters, 14(1985) 1917-20.
[38] I. Batinić-Haberle, I. Spasojević, R.D. Stevens, P. Hambright, I. Fridovich, Manganese(iii) meso-tetrakis(ortho-N-alkylpyridyl)porphyrins. Synthesis, characterization, and catalysis of $O2^{\cdot}-$ dismutation, Journal of the Chemical Society, Dalton Transactions, (2002) 2689-96.
[39] R.A. Baglia, J.P.T. Zaragoza, D.P. Goldberg, Biomimetic reactivity of oxygen-derived manganese and iron porphyrinoid complexes, Chemical Reviews, 117(2017) 13320-52.
[40] Y. Saito, M. Mifune, S. Nakashima, H. Nakayama, J. Odo, Y. Tanaka, et al., Peroxidase-like catalytic activity of anion-exchange resins modified with metalloporphyrins in the dye formation reaction of N, N-Diethylaniline with 4-Aminoantipyrine by hydrogen peroxide., Chem Pharm Bull, 35(1987) 869-72.
[41] Y.G. Mourzina, A. Offenhäusser, Electrochemical properties and biomimetic activity of water-soluble meso-substituted Mn(III) porphyrin complexes in the electrocatalytic reduction of hydrogen peroxide, Journal of Electroanalytical Chemistry, 866 (2020) Article 114159, 10.1016/j.jelechem.2020.114159.
[42] J. Masa, K. Ozoemena, W. Schuhmann, J.H. Zagal, Oxygen reduction reaction using N4-metallomacrocyclic catalysts: fundamentals on rational catalyst design, Journal of Porphyrins and Phthalocyanines, 16(2012) 761-84.
[43] J.H. Zagal, S. Griveau, J.F. Silva, T. Nyokong, F. Bedioui, Metallophthalocyanine-based molecular materials as catalysts for electrochemical reactions, Coordination Chemistry Reviews, 254(2010) 2755-91.
[44] A. Bettelheim, R.J.H. Chen, T. Kuwana, Electroanalysis of oxygen reduction. Part II. Selective redution of hydrogen peroxide or water using polymeric attachment of metalloporphyrins., Journal of Electroanalytical chemistry, 110(1980) 93-102.
[45] Y.O. Su, T. Kuwana, S.-M. Chen, Electrocatalysis of oxygen reduction by water-soluble iron porphyrins: Thermodynamic and kinetic advantage studies, Journal of Electroanalytical Chemistry and Interfacial Electrochemistry, 288(1990) 177-95.
[46] J. Rishpon, S. Gottesfeld, C. Campbell, J. Davey, T.A. Zawodzinski, Amperometric glucose Sensors based on glucose oxidase immobilized in Nafion., Electroanalysis, 6(1994) 17-21.

[47] E. Koposova, A. Kisner, G. Shumilova, Y. Ermolenko, A. Offenhäusser, Y. Mourzina, Oleylamine-stabilized gold nanostructures for bioelectronic assembly. Direct electrochemistry of cytochrome c, Journal of Physical Chemistry C, 117(2013) 13944-51.
[48] T. Mashiko, J.C. Marchon, D.T. Musser, C.A. Reed, M.E. Kastner, W.R. Scheidt, Cytochrome c models, Journal of the American Chemical Society, 101(1979) 3653-5.
[49] G. Battistuzzi, M. Borsari, J.A. Cowan, A. Ranieri, M. Sola, Control of Cytochrome c Redox Potential: Axial Ligation and Protein Environment Effects, Journal of the American Chemical Society, 124(2002) 5315-24.
[50] L. Zhang, K.P. Kepp, J. Ulstrup, J. Zhang, Redox Potentials and Electronic States of Iron Porphyrin IX Adsorbed on Single Crystal Gold Electrode Surfaces, Langmuir, 34(2018) 3610-8.
[51] A. Hughes, D. Grawoig, Statistics: A Foundation for Analysis, USA: Reading: Addison-Wesley; 1971.
[52] F.S. Damos, P. Sotomayor Mdel, L.T. Kubota, S.M. Tanaka, A.A. Tanaka, Iron(III) tetra-(N-methyl-4-pyridyl)-porphyrin as a biomimetic catalyst of horseradish peroxidase on the electrode surface: an amperometric sensor for phenolic compound determinations, Analyst, 128(2003) 255-9.
[53] B. Meunier, J. Bernadou, Active iron-oxo and iron-peroxo species incytochromes P450 and peroxidases, in: B. Meunier (Ed.) Structure and bonding, Springer, Berlin-Heidelberg, 2000, pp. 1-36.
[54] S. Adachi, S. Nagano, K. Ishimori, Y. Watanabe, I. Morishima, T. Egawa, et al., Roles of proximal ligand in heme proteins: replacement of proximal histidine of human myoglobin with cysteine and tyrosine by site-directed mutagenesis as models for P-450, chloroperoxidase, and catalase, Biochemistry, 32(1993) 241-52.
[55] S. Zechel, M.D. Hager, T. Priemel, M.J. Harrington, Healing through Histidine: Bioinspired Pathways to Self-Healing Polymers via Imidazole–Metal Coordination, Biomimetics, 4(2019) 20.
[56] H. Zheng, D.R. Cooper, P.J. Porebski, I.G. Shabalin, K.B. Handing, W. Minor, CheckMyMetal: a macromolecular metal-binding validation tool, Acta Crystallographica Section D, 73(2017) 223-33.
[57] S. Wang, H. Zhai, Z. Chen, H. Wang, X. Tan, G. Sun, et al., Constructing a Sensitive Electrochemical Sensor for Tyrosine Based on Graphene Oxide-ε-MnO2Microspheres/Chitosan Modified Activated Glassy Carbon Electrode, J Electrochem Soc, 164(2017) B758-B66.
[58] S. Zhu, J. Zhang, X.-e. Zhao, H. Wang, G. Xu, J. You, Electrochemical behavior and voltammetric determination of L-tryptophan and L-tyrosine using a glassy carbon electrode modified with single-walled carbon nanohorns, Microchimica Acta, 181(2013) 445-51.
[59] Q. He, Mugadza, Hwang, T. Nyokong, Mechanisms of Electrocatalysis of oxygen reduction by metal porphrins in trifluoromethane sulfonic acid solution, Int J Electrochem Sci, 8(2012) 7045-64.
[60] J.P. Collman, Functional Analogs of Heme Protein Active Sites, Inorganic Chemistry, 36(1997) 5145-55.
[61] ICH Harmonized tripartite guideline. Validation of analytical procedures: text and methodology. Q2(R1).
[62] J.M. Vago, V. Campo Dall'Orto, E. Forzani, J. Hurst, I.N. Rezzano, New bimetallic porphyrin film: An electrocatalytic transducer for hydrogen peroxide reduction, applicable to first-generation oxidase-based biosensors, Sensors and Actuators B: Chemical, 96(2003) 407-12.
[63] J.J. Davis, (ed.), Engeneering the bioelectronic interface: application to analyte biosensing and protein detection, Cambridge, UK: RSC Publishing; 2009.
[64] M.-Q. Wang, Y. Zhang, S.-J. Bao, Y.-N. Yu, C. Ye, Ni(II)-Based Metal-Organic Framework Anchored on Carbon Nanotubes for Highly Sensitive Non-Enzymatic Hydrogen Peroxide Sensing, Electrochimica Acta, 190(2016) 365-70.
[65] L. Yang, C. Xu, W. Ye, W. Liu, An electrochemical sensor for H2O2 based on a new Co-metal-organic framework modified electrode, Sensors and Actuators B: Chemical, 215(2015) 489-96.
[66] Y. Shu, B. Li, Q. Xu, P. Gu, X. Xiao, F. Liu, et al., Cube-like CoSn(OH)6 nanostructure for sensitive electrochemical detection of H2O2 in human serum sample, Sensors and Actuators B: Chemical, 241(2017) 528-33.
[67] C. Xiang, Y. Zou, L.-X. Sun, F. Xu, Direct electrochemistry and enhanced electrocatalysis of horseradish peroxidase based on flowerlike ZnO–gold nanoparticle–Nafion nanocomposite, Sensors and Actuators B: Chemical, 136(2009) 158-62.

[68] L.A. Currie, G. Svehla, Nomenclature for the presentation of results of chemical analysis (IUPAC Recommendations 1994), 66(1994) 595.
[69] H.J. Forman, A. Bernardo, K.J.A. Davies, What is the concentration of hydrogen peroxide in blood and plasma?, Archives of Biochemistry and Biophysics, 603(2016) 48-53.
[70] K.B. O'Brien, S.J. Killoran, R.D. O'Neill, J.P. Lowry, Development and characterization in vitro of a catalase-based biosensor for hydrogen peroxide monitoring, Biosensors and Bioelectronics, 22(2007) 2994-3000.
[71] D.T. Burns, K. Danzer, A. Townshend, Use of the term "recovery" and "apparent recovery" in analytical procedures (IUPAC Recommendations 2002), 74(2002) 2201.
[72] J.E. Frew, P. Jones, G. Scholes, Spectrophotometric determination of hydrogen peroxide and organic hydroperoxides at low concentrations in aqueous solution., Analytica Chimica Acta, 155(1983) 139-50.
[73] A. Nahum, L.D.H. Wood, J.I. Sznajder, Measurement of hydrogen peroxide in plasma and blood, Free Radical Biology and Medicine, 6(1989) 479-84.
[74] S.J. Haswell, (ed.), Practical Guide to chemometrics, USA: Marcel Dekker; 1992.